

Reconstruction of Climate and Environmental Evolution in the Northeastern Tibetan Plateau Since the Holocene Based on Aeolian Sediments

Qingchun Zhang^{1, 2, a}, Fuyuan An^{1, 2, 3, b, *}, Yifan Xu^{1, 2, c}, and Lu Si^{1, 2, d}

¹Key Laboratory of Tibetan Plateau Land Surface Processes and Ecological Conservation (Ministry of Education), Qinghai Normal University, Xining 810008, China;

² Qinghai Province Key Laboratory of Physical Geography and Environmental Process, College of Geographical Science, Qinghai Normal University, Xining 810008, China;

³ Academy of Plateau Science and Sustainability, People's Government of Qinghai Province and Beijing Normal University, Xining 810016, China.

^a2108514042@qq.com, ^b dongzhu8@sina.com, ^c xyfqhu@163.com, ^d 3097003517@qq.com

Abstract. This study aims to elucidate the climatic and environmental evolution and its driving mechanisms in the northeastern Tibetan Plateau since the Holocene. Detailed analysis of the KSH profile, combined with Optically Stimulated Luminescence (OSL) dating and the measurement of environmental indicators, including the mean grain size (Mz) and low-frequency magnetic susceptibility (χ_{lf}), reveals the characteristics of climatic and environmental changes in this region throughout the Holocene. Further, by comparing the environmental indicators from the KSH profile with summer solar insolation at 65°N, annual precipitation reconstructed from pollen data in Gonghai Lake sediments in Northern China, and the GISP2 $\delta^{18}\text{O}$ variation curve from Greenland ice cores, this study categorizes the Holocene climatic and environmental evolution into three stages: a cold and dry early Holocene (11.7-8 ka), transitioning to a warm and humid mid-Holocene (8-4 ka), and returning to a cold and dry climate in the late Holocene (~4 ka to present). The findings indicate that the climatic changes in this area throughout the Holocene are consistent with global climatic trends, with variations in the intensity of the East Asian summer monsoon playing a key role in regional climatic evolution.

Keywords: Holocene; Optically Stimulated Luminescence; Climate change.

1. Introduction

The Holocene epoch, a pivotal period for the evolution of human civilization, is intrinsically linked to the development of modern humans and thus represents a focal point of paleoclimate research[1]. Extensive studies have indicated that the Holocene climate was marked by instability, characterized by numerous oscillations between colder, drier periods and warmer, more humid phases[2]. This period witnessed several abrupt climate events on millennial and centennial scales, which undeniably exerted profound impacts on the contemporary natural environment. Consequently, examining the climatic and environmental evolution during this epoch is of critical importance for predicting future climatic trends and understanding their potential implications for human survival and development. The Loess-Paleosol-Sand sequence, a product of aeolian processes driven by cyclical climatic fluctuations since the Quaternary, encapsulates rich paleoenvironmental data, making it an invaluable proxy for studying Holocene climate dynamics[3]. Numerous scholars have employed a variety of climatic proxies, including grain size, magnetic susceptibility, geochemical elements, color, and clay mineralogy, to conduct comprehensive studies on representative Loess-Paleosol-Sand sequences across different regions. Through the analysis of these climatic proxies, the changing characteristics of these indicators and their environmental implications have been elucidated.

The northeastern Tibetan Plateau, situated on the northwest margin of the Asian monsoon region, is under the combined influence of the Asian summer and winter monsoons and the Westerly winds. This unique geographical setting renders the area particularly sensitive to climatic shifts, making it

an ideal site for regional and even global climate change studies. In recent years, extensive research utilizing grain size, magnetic susceptibility, geochemical elements, pollen, and clay mineralogy as climatic proxies has been undertaken to explore millennial-scale climatic and environmental evolution during the Holocene in the northeastern Tibetan Plateau, focusing on areas such as the Gonghe Basin, Qinghai Lake Basin, and Qaidam Basin[4]. However, the complex interplay of circulatory patterns and the region's distinctive geographical characteristics result in significant environmental variability across different locales within the study area. Moreover, the inherent differences among various climatic proxies and dating methods contribute to ongoing debates regarding Holocene climatic and environmental changes in the northeastern Tibetan Plateau. Some studies suggest that the early Holocene was marked by relatively colder, drier conditions, while others argue for a warmer, more humid climate during the same period. Thus, further research into Holocene climatic and environmental evolution in the northeastern Tibetan Plateau is warranted to augment existing studies. This study focuses on the KSH profile, a typical Loess-Paleosol section in the northeastern Tibetan Plateau, utilizing optically stimulated luminescence (OSL) dating combined with environmental indicators such as grain size and magnetic susceptibility to comprehensively analyze the region's Holocene climatic and environmental changes and unravel the underlying mechanisms driving these transformations.

2. Study area and sampling strategy

2.1 Study area

The KSH profile is located in the northeastern Tibetan Plateau (Figure 1), where it exhibits typical characteristics of a continental plateau climate. The annual mean temperature ranges from -0.9 to 8.5°C, with a significant temperature gradient related to elevation and marked regional differences. Diurnal temperature variations are pronounced, accompanied by abundant sunlight and a monsoonal pattern where heat and rainfall coincide.



Figure 1. Location and topography of the KSH profile

The annual precipitation is 450 mm, with Tongren City receiving an average of 409.1 mm. Precipitation exhibits high variability and uneven spatial and temporal distribution. The evaporation rate is 1.8 to 2.8 times that of the precipitation, with annual sunshine hours totaling 1580. The frost-free period is brief, characterized by distinct cold and warm seasons as well as dry and wet periods, leading to a relatively short vegetation growth period. The grassland ecosystem within this

region is sensitive and fragile. The area hosts over 60 rivers, among which the Longwu River runs longitudinally from north to south, spanning a total length of 144 kilometers.

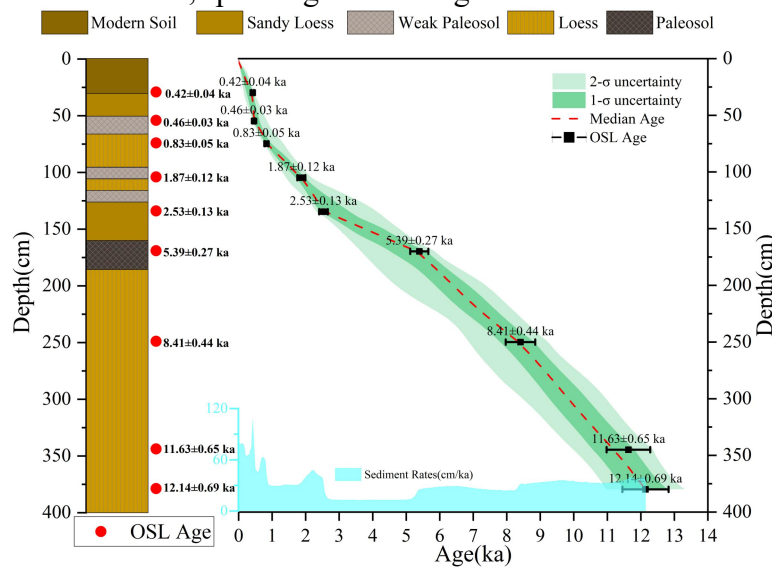


Figure 2. Age-depth modeling of KSH profile

2.2 Sampling strategy

Situated at an elevation of 2922 meters, the KSH profile has a total thickness of 400 cm and is located on the second terrace of a tributary of the Yellow River. The sedimentary sequence of this profile is continuous and undisturbed by stratigraphic disruptions. A total of 81 environmental indicator samples were collected at 5 cm intervals for grain size and magnetic susceptibility analyses. Additionally, optically stimulated luminescence (OSL) samples were collected at nine different depths (30 cm, 55 cm, 75 cm, 105 cm, 135 cm, 170 cm, 250 cm, 345 cm, and 380 cm) for OSL dating. Based on field observations and laboratory analyses, a detailed description of the profile is provided in Figure 2.

3. Methods

3.1 OSL dating

The preparation and analysis of OSL samples from the KSH profile were conducted in the OSL Laboratory within the Key Laboratory of Physical Geography and Environmental Processes, College of Geographic Sciences, Qinghai Normal University. Both sample preparation and instrumental analysis were performed under red light conditions (wavelength 655 ± 30 nm) within a sealed darkroom, in strict accordance with laboratory protocols. This included the proper disposal of waste sand and liquids, ensuring all procedures were conducted away from light, utilizing fume hoods, and wearing protective gear throughout the process. The testing for concentrations of ^{238}U , ^{232}Th , and ^{40}K elements was carried out at the Xi'an Geological Survey Center[5].

3.2 Grain size analysis and magnetic susceptibility measurements

Grain size analysis was completed in the Grain Size Laboratory of the College of Geographic Sciences, Qinghai Normal University, using a Mastersizer 2000 laser diffraction particle size analyzer produced by Malvern Instruments, UK, capable of measuring particle sizes ranging from 0.02 to 2000 μm [6].

Magnetic susceptibility measurements, including both preparation and analysis, were performed in the Pre-treatment Laboratory within the same college. The instrument used was the MS-2 Magnetic Susceptibility Meter manufactured by Bartington Instruments, UK. Samples were tested for both low-frequency magnetic susceptibility (470 Hz) and high-frequency magnetic susceptibility

(4700 Hz). The low-frequency mass-specific magnetic susceptibility (χ_{lf}), high-frequency mass-specific magnetic susceptibility (χ_{hf}), and frequency-dependent magnetic susceptibility (χ_{fd}) of the samples were calculated[7].

4. Result

4.1 Chronological framework

The Optically Stimulated Luminescence (OSL) dating results for the KSH profile samples reveal that the age at the top of the profile is approximately 0.42 ± 0.04 thousand years ago (ka), while the age at the base is determined to be 12.14 ± 0.69 ka. These findings exhibit a robust linear relationship between age and depth across the profile, as illustrated in Figure 2. This linear trend indicates a consistent sedimentation rate over the time span covered by the profile, providing valuable insights into the depositional history and environmental changes within the region during the Holocene epoch.

4.2 Environmental Indicator Results

As illustrated in Figure 3, the grain size analysis of the KSH profile indicates that the mean grain size (Mz) ranges between 19.47 and 35.67 μm , with an average of 24.48 μm . The content of clay particles ($<4 \mu\text{m}$) varies from 8.65 to 14.83 %, averaging 11.94 %. The silt fraction (4–63 μm) exhibits less variation, ranging between 54.92 and 71.67 %, with an average of 65.42 %. The sand fraction ($>63 \mu\text{m}$) varies between 16.93 and 36.43 %, with an average value of 22.64 %. Notably, the clay content is elevated during stages of paleosol development, whereas sand content peaks during loess accumulation phases.

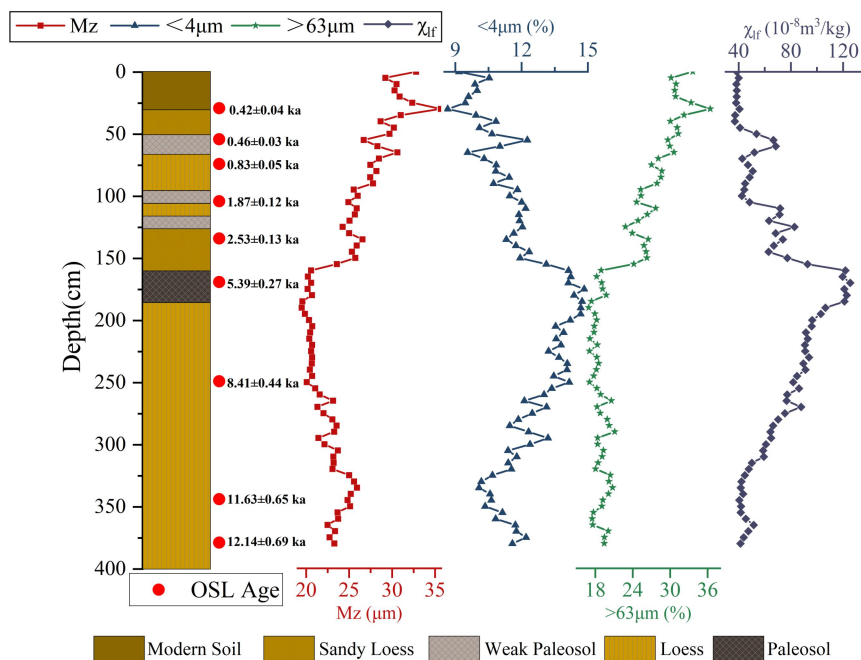


Figure 3. Variation of the Mean Grain Size (Mz), Content of Particles $<4 \mu\text{m}$, Content of Particles $>63 \mu\text{m}$, and Low-Frequency Magnetic Susceptibility (χ_{lf}) with Depth in the KSH Profile

Magnetic susceptibility across the profile shifts significantly with sedimentary layers. The low-frequency magnetic susceptibility (χ_{lf}) ranges from 37.12 to $125.53 \times 10^{-8} \text{ m}^3/\text{kg}$, with a mean of $65.51 \times 10^{-8} \text{ m}^3/\text{kg}$. The content of particles less than $4 \mu\text{m}$ in diameter is relatively higher during periods of paleosol development, correlating well with magnetic susceptibility indicators. The highest values of χ_{lf} are observed during paleosol formation stages, while comparatively lower values are seen during loess development phases. This pattern suggests that climate conditions were

warmer and more humid during periods of paleosol development, facilitating better soil formation and the accumulation of magnetic minerals.

5. Discussion

To elucidate the climatic and environmental evolution and the driving mechanisms in the northeastern Tibetan Plateau since the Holocene, this study compares the mean grain size (Mz), low-frequency magnetic susceptibility (χ_{lf}) from the KSH profile with summer solar insolation at 65°N[8], reconstructed annual precipitation (P_{ANN}) from pollen data in the sediments of Gonghai Lake in Northern China[9], and the Greenland Ice Sheet Project 2 (GISP2) $\delta^{18}O$ variation curve[10] (Figure 4). This comparison allows for the division of the region's Holocene climatic and environmental evolution into three stages.

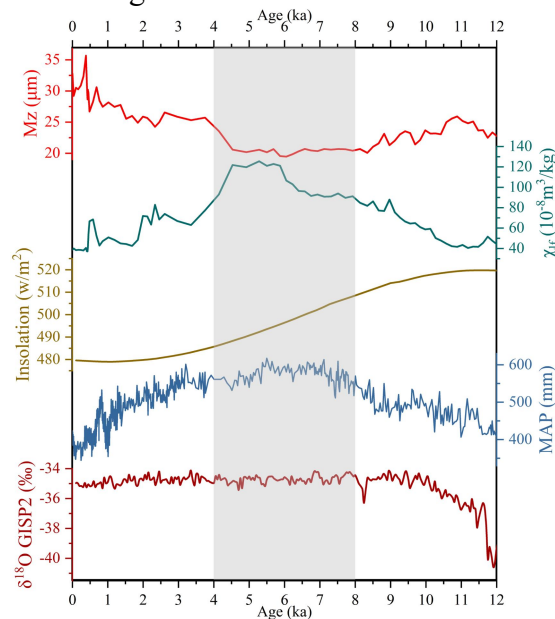


Figure 4. Correlation of Mean Grain Size (Mz) and Low-Frequency Magnetic Susceptibility (χ_{lf}) in the KSH Profile with Summer Solar Insolation at 65°N[8], Annually Reconstructed Precipitation (P_{ANN}) from Gonghai Lake Sediments in Northern China[9], and $\delta^{18}O$ Variations from GISP2 Ice Cores[10]

Stage 1. Early Holocene (11.7-8 ka): During this period, the KSH profile exhibited larger Mz values and lower χ_{lf} values, which gradually increased, indicating a cold and dry climate with weak soil formation processes. High sedimentation rates (Figure 1) suggest active aeolian processes. Both the reconstructed annual precipitation (P_{ANN}) from Gonghai Lake and the GISP2 $\delta^{18}O$ variation curves showed low values, indicating a global climate dominated by cold and dry conditions. The East Asian summer monsoon was weak, insufficient to transport adequate moisture into the northeastern Tibetan Plateau. Simultaneously, high summer solar insolation at 65°N indicates strong evaporation, potentially affecting atmospheric humidity and leading to aridification.

Stage 2. Mid-Holocene (8-4 ka): This stage is characterized by a decrease in the Mz values and an increase in χ_{lf} values of the KSH profile, alongside reduced sedimentation rates. These indicators suggest a warm and humid climate with enhanced soil formation processes in the region. The reconstructed P_{ANN} from Gonghai Lake and the GISP2 $\delta^{18}O$ variation curves both show high values, indicative of a robust East Asian summer monsoon. This confirms that the climate in the northeastern Tibetan Plateau was significantly influenced by the East Asian summer monsoon during this period. A gradual decrease in summer solar insolation at 65°N suggests reduced evaporation, thereby increasing effective humidity in the atmosphere.

Stage 3. Late Holocene (~4 ka to present): During this period, the KSH profile's Mz values increased, and χ_{lf} values rapidly decreased, with higher sedimentation rates, indicating a shift back to a cold and dry climate with weakened soil formation processes and intensified aeolian activity.

The declining trend in the reconstructed P_{ANN} from Gonghai Lake further indicates a trend towards colder and drier climate conditions during this stage.

6. Summary

Based on OSL dating results and environmental indicator analysis from the KSH profile in the northeastern Tibetan Plateau, this study comprehensively examines the climatic and environmental changes in the region since the Holocene. It was found that the region was dominated by a cold and dry climate during the early Holocene, reflecting a phase of weak East Asian summer monsoon within a global climatic context; the climate shifted towards warm and humid conditions in the mid-Holocene, indicating an intensification of the East Asian summer monsoon that brought increased moisture to the northeastern Tibetan Plateau; and returned to cold and dry conditions in the late Holocene, signaling a weakening of the East Asian summer monsoon. By comparing with external climatic indicators, this study confirms the close connection between climatic and environmental evolution in the northeastern Tibetan Plateau with global climatic trends and variations in the intensity of the East Asian summer monsoon. These findings provide important regional evidence for understanding global climatic change patterns since the Holocene and offer a scientific basis for predicting future climatic trends. Further research is needed to explore additional environmental indicators to enhance the accuracy and depth of understanding of climatic and environmental changes in the northeastern Tibetan Plateau since the Holocene.

Acknowledgements

This research was supported by the National Natural Science Foundation of China (NSFC-42371019, 41961014), along with contributions from the Qinghai Provincial Key Laboratory of Salt Lake Geology and Environment (202102) and the Qinghai "Kunlun Talent" Innovation and Entrepreneurship Talent Plan.

References

- [1] Waters C N, Zalasiewicz J, Summerhayes C, et al. The Anthropocene is functionally and stratigraphically distinct from the Holocene[J]. *Science*, 2016, 351(6269): aad2622.
- [2] Schilman B, Bar-Matthews M, Almogi-Labin A, et al. Global climate instability reflected by Eastern Mediterranean marine records during the late Holocene[J]. *Palaeogeography, Palaeoclimatology, Palaeoecology*, 2001, 176(1-4): 157-176.
- [3] Yafeng S, Zhaozheng K, Sumin W, et al. Mid-Holocene climates and environments in China[J]. *Global and Planetary Change*, 1993, 7(1-3): 219-233.
- [4] Qiang M, Jin Y, Liu X, et al. Late Pleistocene and Holocene aeolian sedimentation in Gonghe Basin, northeastern Qinghai-Tibetan Plateau: Variability, processes, and climatic implications[J]. *Quaternary Science Reviews*, 2016, 132: 57-73.
- [5] Murray A, Arnold L J, Buylaert J P, et al. Optically stimulated luminescence dating using quartz[J]. *Nature Reviews Methods Primers*, 2021, 1(1): 72.
- [6] Folk R L. A review of grain-size parameters[J]. *Sedimentology*, 1966, 6(2): 73-93.
- [7] Schenck J F. The role of magnetic susceptibility in magnetic resonance imaging: MRI magnetic compatibility of the first and second kinds[J]. *Medical physics*, 1996, 23(6): 815-850.
- [8] Berger A, Loutre M F. Insolation values for the climate of the last 10 million years[J]. *Quaternary science reviews*, 1991, 10(4): 297-317.
- [9] Chen F, Chen X, Chen J, et al. Holocene vegetation history, precipitation changes and Indian Summer Monsoon evolution documented from sediments of Xingyun Lake, south-west China[J]. *Journal of Quaternary Science*, 2014, 29(7): 661-674.

- [10] Johnsen S J, Dahl-Jensen D, Gundestrup N, et al. Oxygen isotope and palaeotemperature records from six Greenland ice-core stations: Camp Century, Dye-3, GRIP, GISP2, Renland and NorthGRIP[J]. Journal of Quaternary Science: Published for the Quaternary Research Association, 2001, 16(4): 299-307.